Permafrost distribution and conditions at the headwalls of two receding glaciers (Schladminger and Hallstadt glaciers) in the Dachstein Massif, Northern Calcareous Alps, Austria

Matthias Rode[1], Harald Schnepfleitner[1], Oliver Sass[2], Andreas Kellerer-Pirklbauer[1] and Christoph Gitschthaler[1]

[1]Department of Geography and Regional Science, Working Group on Alpine Landscape Dynamics (ALADYN), University of Graz
[2]Institute of Geography, Working Group on Geomorphology, University of Bayreuth

Correspondence to: A. Kellerer-Pirklbauer (andreas.kellerer@uni-graz.at)

Abstract. Permafrost distribution in rockwalls surrounding receding glaciers is an important factor for rock slope failure and rockwall retreat. The Northern Calcareous Alps of the Eastern European Alps form a geological and climatological transition zone between the Alpine Foreland and the Central Alps. Some of highest summits of this area are located in the Dachstein Massif (47°28'32″N, 13°36'23″E) in Austria reaching up to 2995 m a.s.l. Occurrence, thickness and thermal regime of permafrost at this partly glaciated mountain massif are scarcely known and related knowledge is primarily based on regional modeling approaches. We applied a multi-method approach with continuous ground surface and near-surface temperature monitoring, measurement of bottom temperature of the winter snow cover, electrical resistivity tomography (ERT), airborne photogrammetry, topographic maps, visual observations and field mapping for permafrost assessment. Our research focused on steep rockwalls consisting of massive limestone above several receding glaciers exposed to different slope aspects at elevations between c.2600-2700 m a.s.l. We aimed to quantify distribution and conditions of bedrock permafrost particularly at the transition zone between the present glacier surface and the adjacent rockwalls.

Low ground temperature data suggest that permafrost is mainly found at cold, north exposed rockwalls. At southeast exposed rockwalls permafrost is only expected in very favourable cold conditions at shadowed higher elevations (2700 m a.s.l.). ERT measurements reveal high resistivities (>30.000 ohm.m) at ≥1.5 m depth at north-exposed slopes (highest measured resistivity values > 100 kohm.m). Based on laboratory studies and additional measurements with small scale ERT, these values indicate permafrost existence. Such permafrost bodies were found in the rockwalls at all measurement sites independent of investigated slope orientation. ERT data indicate large permafrost bodies at north exposed sites whereas discontinuous permafrost bodies prevail at northwest and northeast facing rockwalls. In summary, permafrost distribution and conditions around the headwalls of the glaciers of the Dachstein Massif is primarily restricted to the north exposed sector, whereas at the south exposed sector permafrost is restricted to the summit region.

Keywords: Dachstein, Eastern Alps, permafrost, electrical resistivity tomography, base temperature of the winter snow cover, ground surface temperature

1 Introduction

Climate change has a great impact on perennially frozen and glaciated high mountain regions (Haeberli and Hoelzle, 1995; Haeberli et al., 1997; Harris et al., 2001; Lieb et al., 2012). Glacier retreat (Paul et al., 2004; Zemp et al., 2006; Kellerer-Pirklbauer et al., 2008) is the visible evidence with a loss of estimated 50% of the original glacier volume in the European Alps between the end of the Little Ice Age around 1850 and 1975, 10% in 1975-2000 and further 10% in 2000-2009 (Haeberli et al., 2007, 2013, Magnin et al. 2017).

Invisible, but also measurable, are permafrost changes in the subsurface. Once glacier-covered rock surfaces with former temperatures around the melting point – conditioned by temperate glacier ice – become subjected to direct local atmospheric conditions after the ice melted. Depending on slope orientation and shading effects of these rock surfaces permafrost aggradation is possible at such sites after exposure. However, in case of cold and polythermal glaciers (with cold ice restricted to cold, high-altitude parts of the glacier; Benn and Evans, 2010) permafrost might exist even below glacier-covered areas. In addition to that, cirque glaciers (and also those in our study area) are commonly separated from the headwall by a distinct crevasse (randkluft). Air can enter into this crevasse allowing a better coupling of the air and bedrock even below the glacier surfaces and more efficient cooling during the autumn season. Therefore, both a polythermal glacier and a glacier with a distinct randkluft might allow permafrost aggregation below the glacier surface.

Changes in ground thermal conditions, permafrost extent and hydrology are all sensitive to predicted future climate change (Gobiet et al., 2014). A warming of about 0.5 to 0.8°C in the upper tens of meters of alpine permafrost between 2600 and 3400 m a.s.l at the European alps in the last century (Harris et al., 2003) effects in a vertical mean rise of the lower limit of permafrost by about 1m/year (Frauenfelder, 2005). This can potentially trigger rockwall instabilities (Wegmann et al., 1998; Sattler et al., 2011; Ravanel and Deline, 2011; Kellerer-Pirklbauer et al., 2012; Krautblatter et al., 2013; Draebing et al., 2017a, b). Therefore, acquiring knowledge on the permafrost distribution and freezing and thawing in the active layer (Supper et al., 2014) is important in high mountain areas particularly if infrastructure is potentially threatened (Kern et al. 2012). While ground surface temperature measurements in rockwalls (e.g. Matsuoka and Sakai, 1999; Gruber et al., 2003; Kellerer-Pirklbauer, 2017) can provide valuable point information on rock temperature and thermal conditions of permafrost, geophysical techniques enable the visualization of subsurface permafrost characteristics in 2D- or 3D-arrays. Several authors used electrical resistivity tomography (ERT) for permafrost investigations in sediments (e.g. Kneisel et al., 2008; Hauck, 2001; Hauck et al., 2003; Marescot et al., 2003; Laxton and Coates, 2011; Rödder and Kneisel, 2012; Stiegler et al., 2014). In contrast, in rockwalls comparable measurements are relatively scarce (e.g. Krautblatter and Hauck, 2007; Hartmeyer et al., 2012; Magnin et al., 2015, Draebing et al. 2017a, b) and for rockwalls close above the present glacier surfaces (Supper et al., 2014), ERT data are widely missing. Accordingly, the aims of this study are to detect, delimit and characterize permafrost in the rockwalls surrounding the retreating Schladminger and Hallstatt glaciers in the Dachstein area and thus, to contribute to the question how widespread glacier retreat will affect permafrost degradation and/or aggradation.

2 Study Area

2.1 General Setting

The Dachstein Massif with its highest peak, the Hoher Dachstein (2995m a.s.l.) located at 47°28'32″N and 13°36'23″E, are a mountain range in the Northern Calcareous Alps in Austria covering an area of about 400 km^2 (Fig. 1). The study area is characterized by steep rockwalls (e.g. Dachstein south wall with 850 m altitude difference within a vertical distance of some hundred meters) towering relatively flat, glacier-covered plateaus and extensive touristic infrastructure with cable cars, ski lifts and ski runs. In particular the Schladming Glacier (Fig. 1) is intensively used for alpine skiing. The surrounding headwalls are also partly used by means of a military transmitting station, lift stations and public climbing routes.

The prevailing rock type in the study area is the very compact Dachstein Limestone (GBA, 1982*;* Gasser et al., 2009). The climatic conditions of the study area are dominated by west and northeast air flows. The main maximum of precipitation is during summer with a secondary maximum in winter. Air temperature measurements at the surface of the Schladming Glacier next to the Hunerkogel at 2600 m a.s.l. showed annual average temperatures (MAAT) of -2.4°C from 2007-2016.

The MAAT of -2.4°C (2007-2016) at about 2600 m a.s.l. at the Dachstein massif indicates the possible presence of discontinuous permafrost in the study area (Humlum, 1998). The first evidence of the existence of permafrost in the study area was provided by bottom temperature measurements of the snow cover (BTS) carried out by Schopper (1989) and Lieb and Schopper (1991) in the proglacial area of the Schladming glacier at 2300-2400 m a.s.l. According to these authors, the lower limit of discontinuous permafrost can be expected at this elevation. More recent simulations regarding the probability of permafrost existence in Austria (Ebohon and Schrott, 2009) or in the entire European Alps (Boeckli et al., 2012 a, b) revealed that permafrost existence in the study area is particularly likely at north-exposed, higher elevated slopes as well as in the proglacial area of the Schladminger Glacier.

Our research focused on the lower parts of steep rockwalls at four different measurement sites (MS) at elevations between 2600-2700 m a.s.l. next to the Schladminger and Hallstatt glaciers (Fig. 1). The Koppenkarstein site (MS-K; summit elevation 2863 m a.s.l) was chosen due to the high probability of permafrost at this shaded position, the pronounced randkluft and the well-documented, high amount of glacier surface lowering. The Dirndln site (MS-D) was selected because of a distinct blowout depression between the glacier and the mountain (Fig. 2). This causes snow-poor and ice-free conditions at the footslope of the mountain which probably reduced ice coverage even during the LIA extent of the glacier. The Gjaidstein site (MS-G) is slightly lower and oriented to the west which makes permafrost occurrence less probable. At Hunerkogel (MS-H) the cable car station is located which makes this site interesting in terms of endangered infrastructure. There are no sites oriented to the south as there is only a very small glacier and the probability of permafrost is much lower.

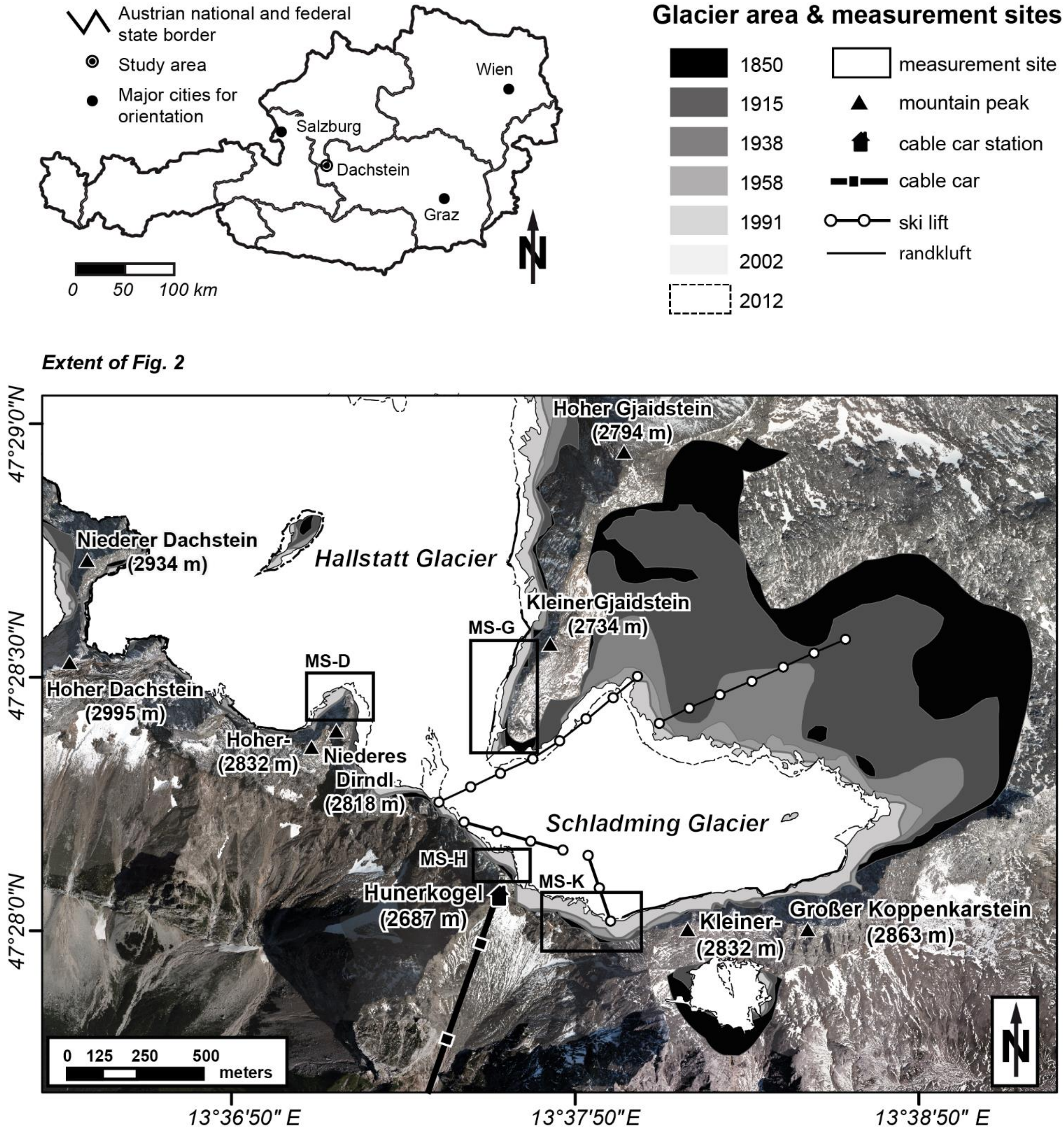

Figure 1: Location of the study area Dachstein Massif in Austria and an overview map depicting the four different measurement sites within the study area. Glacier recession between c.1850 (LIA maximum) and 2012 is indicated. Abbreviations: MS-D: measurement site Dirndln; MS-G: Gjaidstein; MS-H: Hunerkogel; MS-K: Koppenkarstein. Orthophoto in the background by Province of Upper Austria 2013.

2.2 Reconstruction of deglaciation

The Hallstadt Glacier and the Schladming Glacier have been subject to substantial mass loss and glacier surface lowering since the Little Ice Age/LIA (c.1850) and particularly in the last decades. Hallstatt Glacier lost about 50% of its area and 52% of its length, whereas Schladming Glacier melted down by 55% (area) and 48% (length). The retreat of the glaciers located at the Dachstein Massif since the LIA are well documented by Simony (1895), Moser (1997), Krobath and Lieb (2004), Helfricht (2009) or Fischer et al. (2015). New ice-free areas in the glacier forefield and the surrounding head walls afforded new touristic concepts and safety precautions over the years. A randkluft exists at several places in the study area (see Fig. 1) and is commonly visible during the ablation season. The total length of the mapped randkluft in the area depicted in Fig. 1 is 2841 m, which is about 14,9 % of the total glacier boundary in this map.

In addition to the abovementioned published glacier reconstructions, airborne photogrammetry, topographic maps, visual observations and field mapping were applied for the reconstruction of deglaciation at our measurement sites. To visualize the vertical changes of the glacier surface, digital terrain models (DTM) with a spatial resolution of 5 m were produced from published 1:25,000 maps of the German-Austrian Alpine Society from 1915 and 2002 by digitizing the 10 m contour lines and generating DTMs using the ArcGIS 10.0 Topo-to-Raster function. The difference between both models showed the glacier retreat of 1915 to 2002. In addition, recent orthophotos from 2009 (provided by the Federal Government of Upper Austria) and data from the third Austrian glacier inventory (Fischer et al., 2015) enabled the mapping of the present glacier surface and thus, the estimation of glacier retreat from 1915 to 2009. The comparison of historic photographs from 1958 (Schneider, July 1958 from Österreichischer Alpenverein 1958) and own photographs from 2013-2015 gave further information about the vertical surface lowering (Fig. 2).

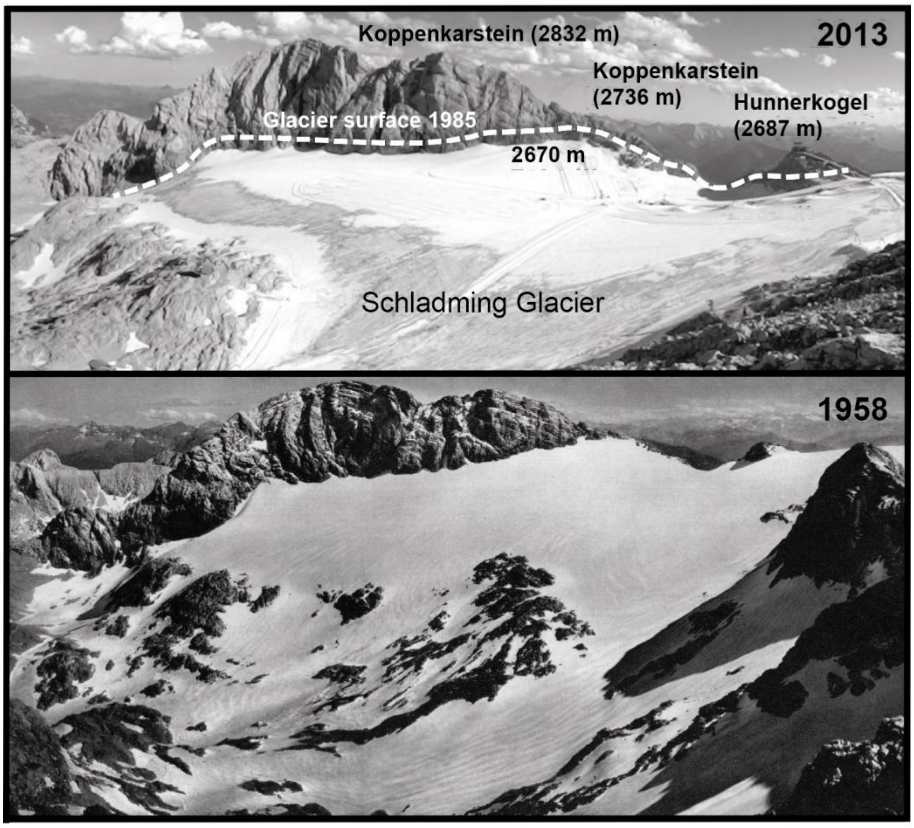

Figure 2: Comparison of the glacier surface at the foot of the Koppenkarstein in 2013 (photo Gitschthaler, 02-08-2013) and 1958 (photo Schneider, July 1958 from Österreichischer Alpenverein 1958). Note the obvious surface change at Hunerkogel. Note that the shooting location of both years is not exactly the same.

The ascertained horizontal recession and vertical surface lowering rates of the glacier area between 1915 and 2009 for the four measurements sites is shown in Table 2. For the MS-K the horizontal recession is about 20 m near the Austriascharte but only 5-10 m at the north face of the Koppenkarstein. The vertical loss there is about 15-20 m. Similar amounts of vertical decline were estimated for the area around the Hunerkogel (MS-H) (cf. Fig. 4), the horizontal recession amounts to 15-30 m. For MS-D the horizontal recession is about 20-50 m, vertically the glacier has lost 5-25 m with highest amounts in northwest exposition. Around the Gjaidstein (MS-G), maximum decline rates, both horizontal (up to 70 m) and vertical (15-35 m), were determined.

Table 2: Horizontal recession and vertical surface lowering rates of the glacier areas in the four sub-regions of interest (Fig. 1) between 1915 and 2009

Measurement site	MS-K	MS-H	MS-D	MS-G
Horizontal decline [m]	5-20	15-30	20-50	20-70
Vertical decline [m]	15-20	15-20	5-25	5-50

3 Methods

We focused on the permafrost distribution in the areas of glacier retreat between 1915 and 2009 (Fig. 2). To this end, we followed a multidisciplinary approach including continuous ground surface temperature (GST) monitoring at the surface using miniature temperature datalogger, bottom temperature of the winter snow cover (BTS; Haeberli, 1973) and electrical resistivity tomography (ERT) profiling.

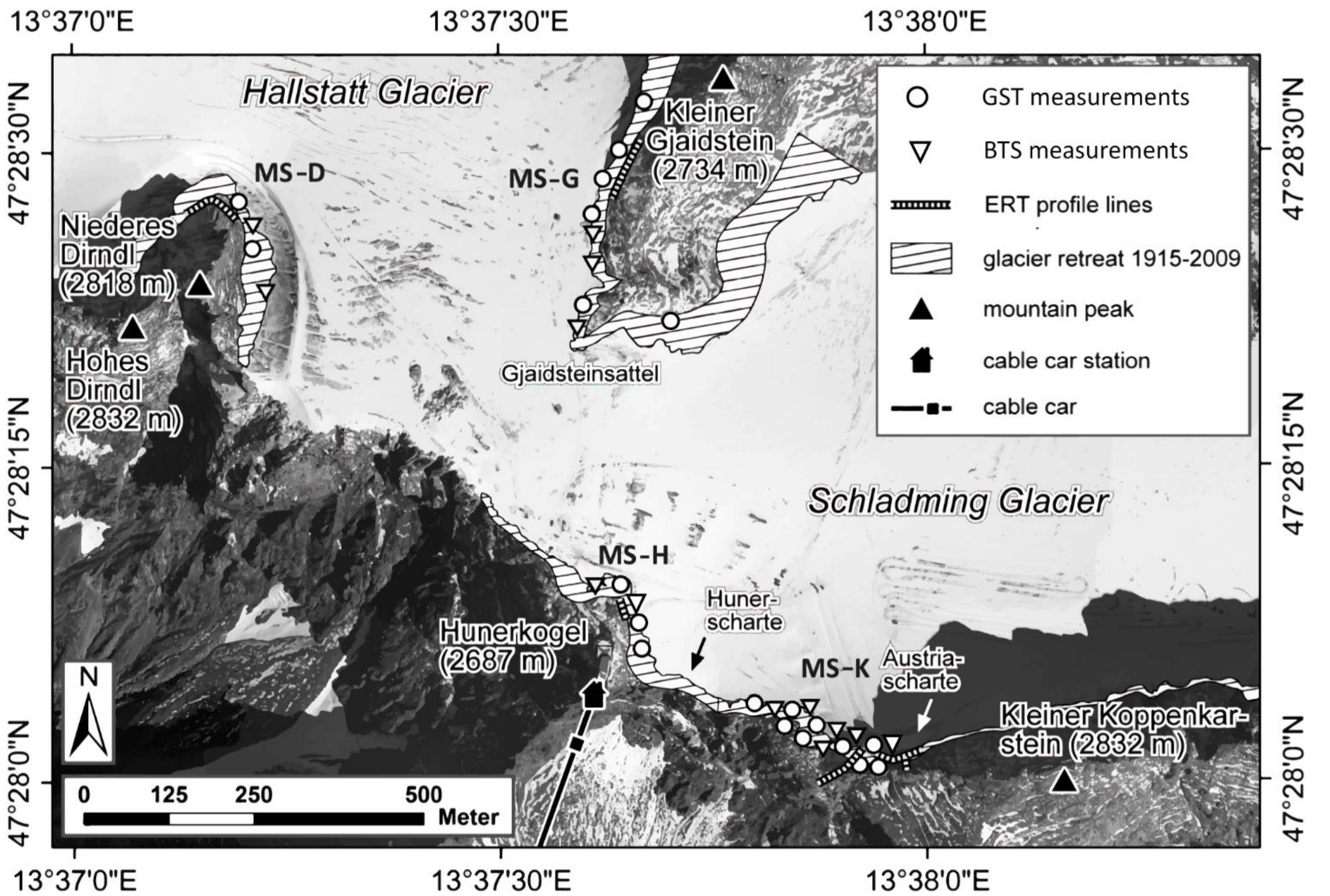

Figure 3: Measurement locations of the different techniques (BTS, GST, ERT) at the studied rockwalls. Data source: Orthophoto by Province of Upper Austria 2013

3.1 Base temperature of the winter snow cover (BTS)

BTS is based on the insulating properties of sufficiently thick snow cover (> 1 m), which prevents the ground surface from short-term periodical variations in air temperature (Haeberli, 1973, 1975). BTS is controlled by the heat flow of the subsurface and is distinctly lower above frozen ground. Haeberli (1973) defined temperatures < -3°C as permafrost areas, measurements between -2°C and -3 °C as uncertainty range and temperatures > -2°C as non-permafrost areas. A self-constructed BTS thermocouple probe with a Pt100 (1/3 DIN class B) fixed to the bottom of a 3 m long steel rod (System KRONEIS, Vienna) at the lower end of a 3 m carbon tube was used. Measurements were performed at each point until constant temperature was registered for at least 2 minutes. The accuracy of measurements depends on several factors like calibration of the temperature sensor or disturbance of the temperature field by the breakthrough of the snow field by the probe. A total of 13 BTS-points (at each point three measurements within an area of 2 m²; cf. Brenning et al., 2005) were determined at recently glacier free areas based on the multitemporal analyses of published maps and orthophotos (Fig. 2) in 2600 – 2700 m a.s.l. In the time period around the measurement date (20-03 to 21-03-2013), the snow cover recorded by a weather station at the Hunerkogel (snowreporter, 2013) increased continuously from 1.5 m (01-12-2012) to 3.5 m (25-03-2013). During the 13 BTS measurements snow depths ranged from 2 to 3.5 m. As pointed out by Brenning et al. (2005), BTS has to be interpreted as a relative measure of ground thermal state and not strictly as a permafrost indicator.

3.2 Ground surface temperature (GST)

To avoid the restrictions of short BTS measurements, additional miniature temperature data loggers (iButtons, e.g. Gubler et al., 2011) were mounted at the bedrock surface. iButtons of type DS1922L, (Maxim Integrated) with a resolution of 0.5 °C and a measurement interval of 1 h were chosen. The sensors were placed in 20 very shallow boreholes with a depth of 2 cm (Fig. 2). Additional protection against moisture was provided by small plastic bags. Preliminary laboratory calibrations of the sensors did not show any effects of the used plastic bags. iButtons where placed at the measurement sites at the rock surface beneath the snow pack on 01-01-2013 and removed on 31-07-2013. Therefore, up to 7 months of data were available for analysis.

With GST it is possible to monitor the seasonal temperature fluctuations at the uppermost centimeters of the surface (e.g. Ishikawa, 2003). The winter equilibrium temperature (WEqT) describes temperature fluxes beneath the snow pack and is defined as the mean temperature of stable conditions during February and March. In case of strong temperature fluctuations – for instance related to atmospheric influence – during this period, the WEqT-approach is not applicable. As with BTS, strongly negative WEqT (< -3°C) are measured on frozen ground (permafrost areas) whereas on non-frozen bedrock the WEqT is usually close to 0°C or moderately negative. Another important parameter is the zero curtain period with temperatures around 0°C caused by the melting of the snow and isothermal conditions within the snow pack. The zero curtain period is framed by the basal-ripening date (RD), which describes the heating of the frozen ground by melting snow and the melt out date (MD), on which the snow cover is gone (Schmid et al., 2012).

3.3 ERT

For geophysical resistivity measurements, a constant current is applied into the ground through two ’current electrodes’ and the resulting voltage differences at two ‘potential electrodes’ are measured (Knödel et al., 2005). From the current and voltage values, an apparent resistivity value is calculated. ERT is excellently suited for permafrost detection as frozen ground is generally characterised by high electrical resistivity (due to the lack of conducting liquid water) and a strong contrast to the unfrozen surrounding (Hauck and Kneisel, 2008; Schrott and Sass, 2008). To determine the true subsurface resistivity in different zones or layers, an ’inversion‘ of the measured apparent resistivity must be carried out; we used the Res2Dinv software package by Loke (1999). A GeoTom-2D system (Geolog2000, Starnberg, Germany) with multicore cables was used. Depending upon the local topography, between 24 and 50 electrodes were used. The connection between the electrodes and the rock was established by stainless steel screws, 12 mm in diameter, which were driven into 12 mm wide shallow boreholes, 50 mm deep and the spacing between two electrodes was 2 m. Thus, the total extent of the survey lines was between 32 and 98 m. Salt water and metallic grease were used to improve electrical contacts. Figure 2 shows the positions of the ERT measurements at rockwall MS-K, MS-H, MS-D and MS-G. The measurements were carried out by means of Wenner array which provides a particularly sound depth resolution in the central parts of the profile (Knödel et al., 2005; Loke, 1999). We used the robust inversion modelling process. The model discretization was set to use an extended model with an increase factor of model depth range of 1.5. Robust inversion delivered very good results in terms of low absolute error (maximum 15.5%). To assess the quality of the results the depth of investigation (DOI) method was used (Oldenburg and Li, 1999; Hilbich et al., 2009; Stiegler et al., 2014). With this technique two inversions of the same data sets are carried out using equation (1), but with two different reference models with homogeneous resistivity values m_{01} and m_{02} (Hilbich et al., 2009). The first reference value (m_1) is usually calculated from the average of the logarithm of the observed apparent resistivity values. The second reference resistivity value (m_2) is usually set at 10 times this value. Model regions with DOI index values >0.2 are considered as unreliable (Hilbich et al., 2009). This empirical method determines the effective depth of investigation (Angelopoulos et al., 2013).

$$DOI(x,y) = \frac{m_1(x,z) - m_2(x,z)}{(m_{01} - m_{02})}, \quad (1)$$

Inversion artefacts are often caused by high resistivities and high resistivity contrasts between frozen and unfrozen subsurfaces and can lead to misinterpretations of the inversion model tomograms. Applying synthetic modelling can be used to confirm the hypotheses drawn from the observed internal permafrost structure of the rockwall. By using the software Res2Dmod (Loke, 1999) simulated data of the expected apparent resistivities were calculated with the same measurement setup as in the field. 5 % Gaussian noise was added to the apparent resistivities to simulate field conditions (Hauck, 2001; Stiegler et al., 2014). The robust inverted synthetic model was compared to the real inverted data. The modelling process continued until both inverted data sets had similar tomograms. The final synthetic model was used as a possible representation of the subsurface (Hilbich et al., 2009; Stiegler et.al., 2014).

3.3.1 Resistivity category definition

To determine the thermal condition within the rockwall the resistivity values have to be grouped into different categories. In this study the results of a small-scale geoelectric monitoring station used for rock moisture and frost weathering research nearby to the ERT-profiles at the Koppenkarstein (Fig. 2, MS-K) were used to classify the resistivities. The same GeoTom-2D system with multicore cables for 68 electrodes was used. The connection to the rock was established by stainless steel screws, 5 mm in diameter, which were driven into 4 mm boreholes, 1 cm deep and 6 cm apart. Thus, the total extent of the survey line was 4.08 m. Additional temperature sensors (Pt1000, Geoprecision) at 0, 2, 6, 12 and 18 cm depth gave simultaneous information about the temperature behaviour within the rock. The combined analysis of resistivity and temperature changes at different depths caused by freeze thaw events provides the necessary information to define the rock resistivity characteristics at different temperatures. The mean resistivities along the whole profile at 2, 6, 12 and 18cm depth were compared with the temperature readings. Similar to the laboratory results of Krautblatter et al. (2010), a rapid increase in resistivity from 13 kohm.m to 30 kohm.m was observed in the temperature range between -0.5 and -1°C (Fig. 3). The unfrozen rock was characterized by resistivities of up to 13 kohm.m, the transition zone with still unfrozen layers ranged from 13-30 kohm.m and frozen rock had resistivities exceeding 30 kohm.m. Similar thresholds were used by Krautblatter et al. (2007) and Magnin et al. (2017).

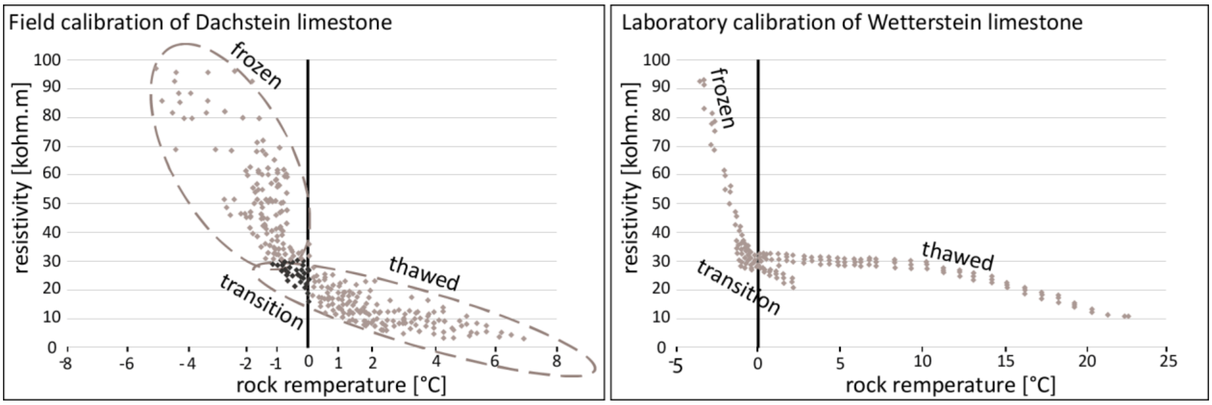

Figure 4: Comparison of small scale ERT (left) and laboratory (right; Krautblatter et al. 2010) calibration measurements.

4 Results

4.1 BTS and GST

The temperature curves from January to July 2013 display that the winter equilibrium temperature (WEqT), as an indicator for permafrost, could be measured at all sites, as well as the zero curtain, RD and MD (Figure 5). At the north exposed MS-K the mean WEqT of nine GST measurements is -3.9°C, the mean of the six BTS measurements is -5.0°C. At MS-H the WEqT (iB-H2) and BTS in northeast aspect is with -5.2°C resp. -5.6°C significantly lower than the measured values at the east exposed rockwall. There, the mean WEqT (iB-H1, iB-H3) is -3.1°C, the mean of the BTS values is even higher (-2.2°C, maximum value of all temperature measurements). At MS-D the mean WEqT of the two iButtons in northeast exposure is -3.6°C while the mean BTS, measured north exposed, is -4.2°C. For MS-G the results show some more fluctuation in temperature at the beginning of the year (iB-G1, February), probably because of less insulation due to a shallow snowpack. Mean WEqT of all GST measurements carried out at the foot of the west to northwest exposed slope is -4.3°C, the mean BTS is -4.5°C. The WEqT of the southeast exposed iB-G2 is more than 1 K higher (-2.9°C), which can be explained by much higher direct solar radiation.

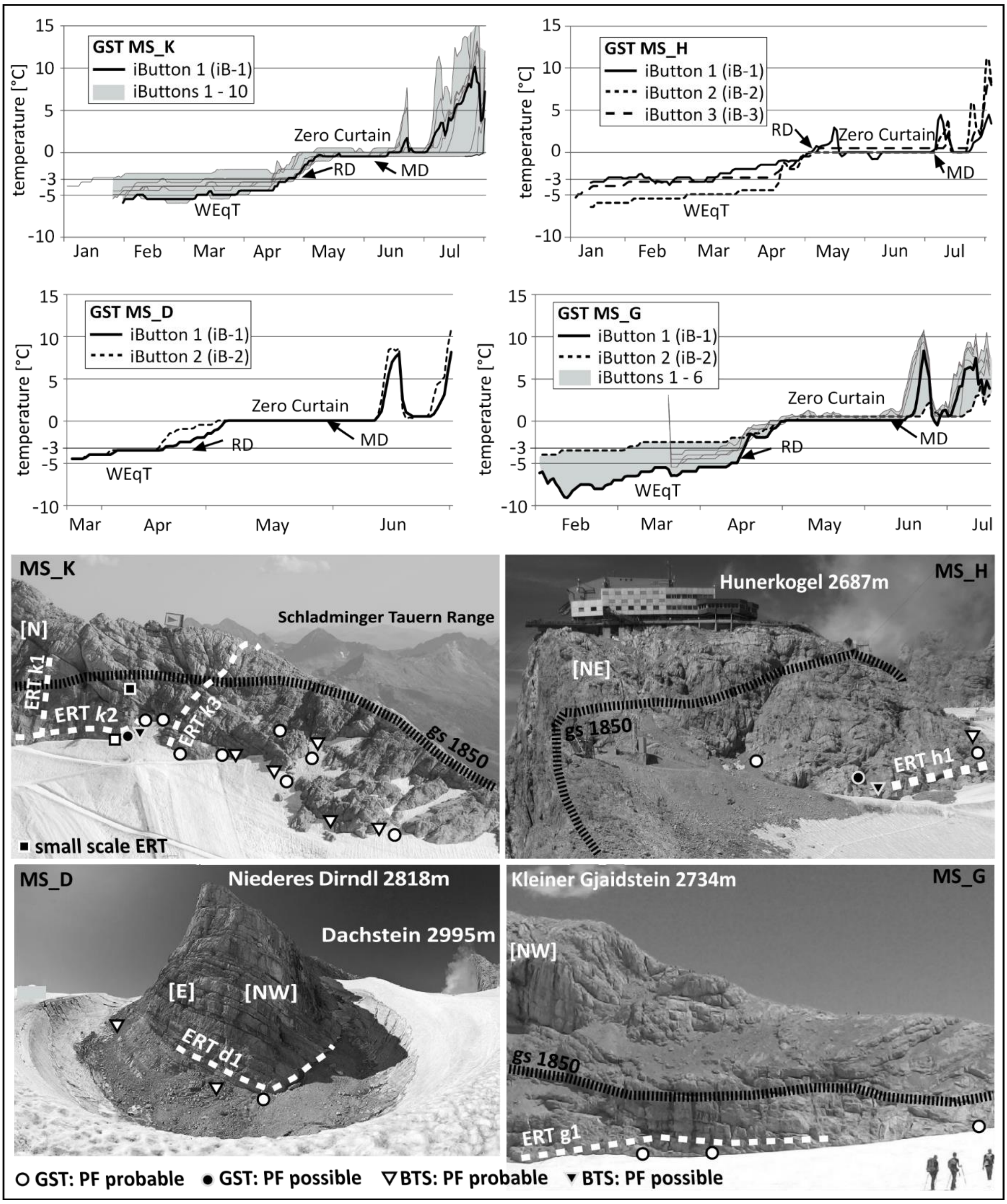

Figure 5: GST measurements from January 2013 to July 2013 and measurement locations of the different techniques at the studied rockwalls including interpretation of results of the GST and BTS measurements. The position of the glacier surface (gs) during the maximum of the LIA is indicated at all four sites. Abbreviations: WEqT = winter equilibrium temperature; RD = basal-ripening date; MD = melt-out date; gs = glacier surface; PF = permafrost. Image data sources: Orthophoto by Province of Upper Austria 2013, terrestrial image of Niederes Dirndl by www.swisseduc.ch

4.2 ERT

Table 1 gives an overview of the 6 ERT profiles and their respective range of resistivities. The temperature/resistivity classification from Fig. 3 constitutes the base for the interpretation of permafrost existence.

Table 1: Parameters and resistivity range of the ERT profiles (05.09.-09.09.2013). PF = permafrost.

code	elevation [m a.s.l]	length [m]	alignment	resistivity [kohm.m]	PF

MS-K1	2640 - 2680	48	vertical	7 - 500	yes
MS-K2	2640	80	horizontal	4 - 330	yes
MS-K3	2635 - 2700	92	vertical	5 - 300	yes
MS-H1	2620	32	horizontal	9 - 160	yes
MS-D1	2630	98	horizontal	7 - 300	yes
MS-G1	2580	98	horizontal	4 - 300	yes

In Fig. 6 all ERT profiles use the same specific resistivity scaling delineating the three possible thermal conditions. At MS-D, wide areas of high resistivities (> 30 kohm.m) are recognizable beneath 1.5 m depth. There are also two pronounced zones with resistivities of more than 100 kohm.m. At MS-G, layers with resistivities between 10 and 20 kohm.m are widespread below 1 m depth. Compared to MS-D the resistivities are lower and more heterogeneous with only two zones of resistivities above 30 kohm.m. At MS-H, only a short ERT profile was possible because of numerous lightning rods installed at the rockwall for the protection of the lift station. Nevertheless, an increase of resistivity is observable with rock depth; beneath 2 m depth the resistivities are between 30 and 80 kohm.m. At the north face of MS-K three ERT profiles were installed, two of them in vertical settings. These two profiles cross the line where the glacier surface was located during the LIA maximum. The resistivity distribution at ERT profile line K3 with a length of 92 m and a penetration depth of almost 20 m shows higher resistivities (>30 kohm.m) in the upper part and lower resistivities in the lower part (10 – 30 kohm.m). In the center of the profile line below 2 m depth, resistivities of more than 100 kohm.m were observed. At profile line K1, higher mean resistivities were measured. The part above the 1850 glacier surface shows resistivities of 30 – 50 kohm.m even at the surface, while below the 1850 line it is in the range between 5 – 20 kohm.m. Below 2-5 m rock depth a massive zone of very high resistivity (>100 kohm.m) is found. The horizontal profile K2 was measured just above the present glacier surface. Like at the other three horizontal profiles, resistivity steeply increases with depth. In the middle of the profile the surface appears to be frozen (>30 kohm.m) with resistivities increasing to >100 kohm.m at ca. 3-7 m depth. The DOI indexes prove the reliability of all data sets to depths of about 10-15 m (DOI mostly <0.2). The absolute error values of all inversions are between 6.5 % and 15.5 %.

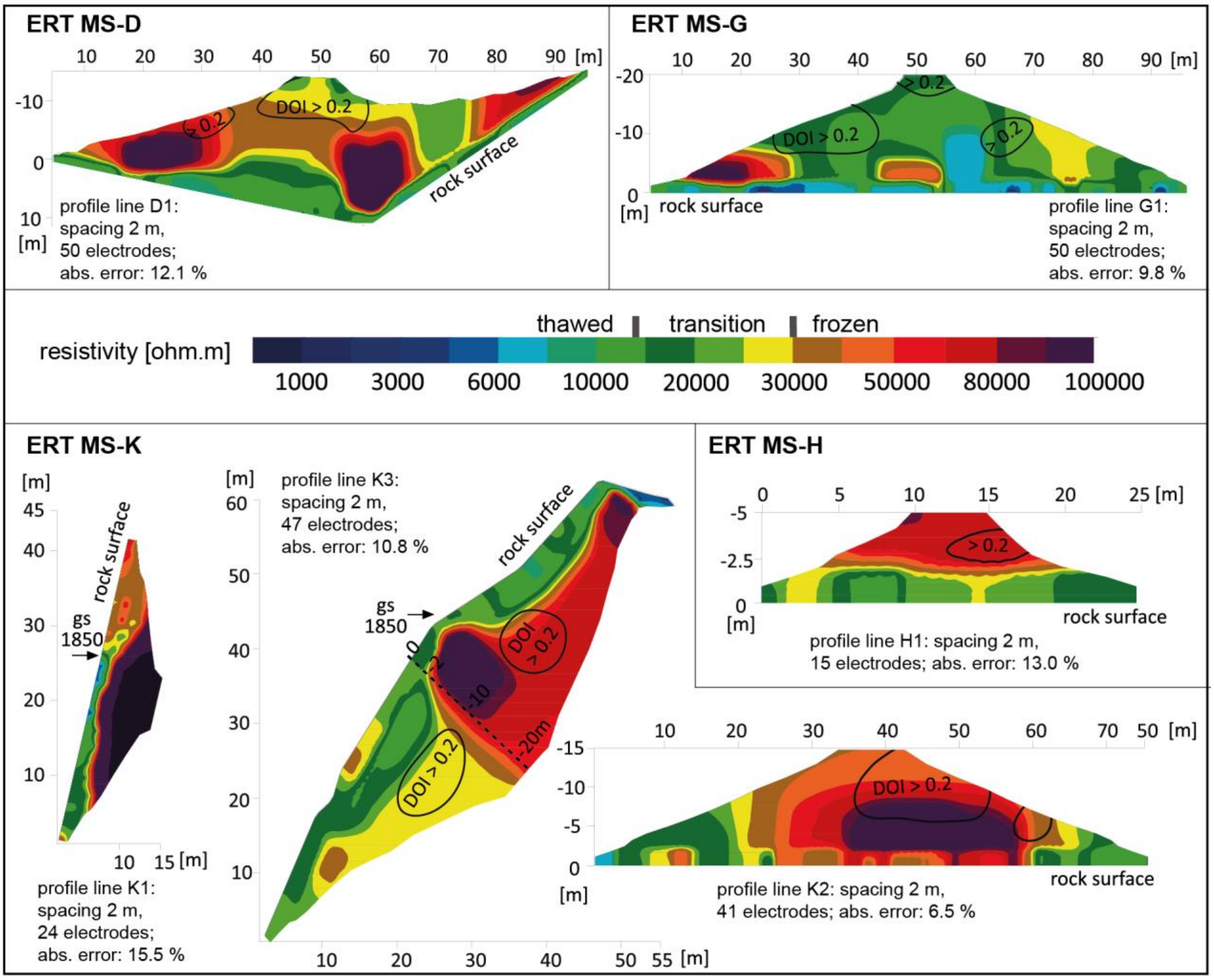

Figure 6: ERT results at MS-D (measurement site Dirndln), MS-G (Gjaidstein), MS-K (Koppenkarstein) and MS-H (Hunerkogel). gs 1850 = glacier surface at c. 1850

Boxplot diagrams dividing the ERT profiles into 1 m depth sections are shown in Fig. 7. The profile MS-G is the only one with mean and medium resistivities below the 30 kohm.m threshold at all depths. In all other recorded profiles, mean values of >30 kohm.m are reached below a certain depth, which is approx. 3 m at MS-D, MS-H and MS-K1, and 4-5 m at MS-K3. The profile MS-K2 is the only one with mean and median values of ca. 30 kohm.m even in the outermost layer. The resistivity increase at MS-K1 between 2 and 3 m is particularly pronounced; at ≥3 m, 100% of the values are above the 30 kohm.m threshold pointing to a well-defined permafrost table. At greater depth (approx. 5-8 m) mean values of 80 – 100 kohm.m are reached at MS-D, MS-K1 and MS-K2, while the mean is at around 60 kohm.m at MS-K3 and MS-H.

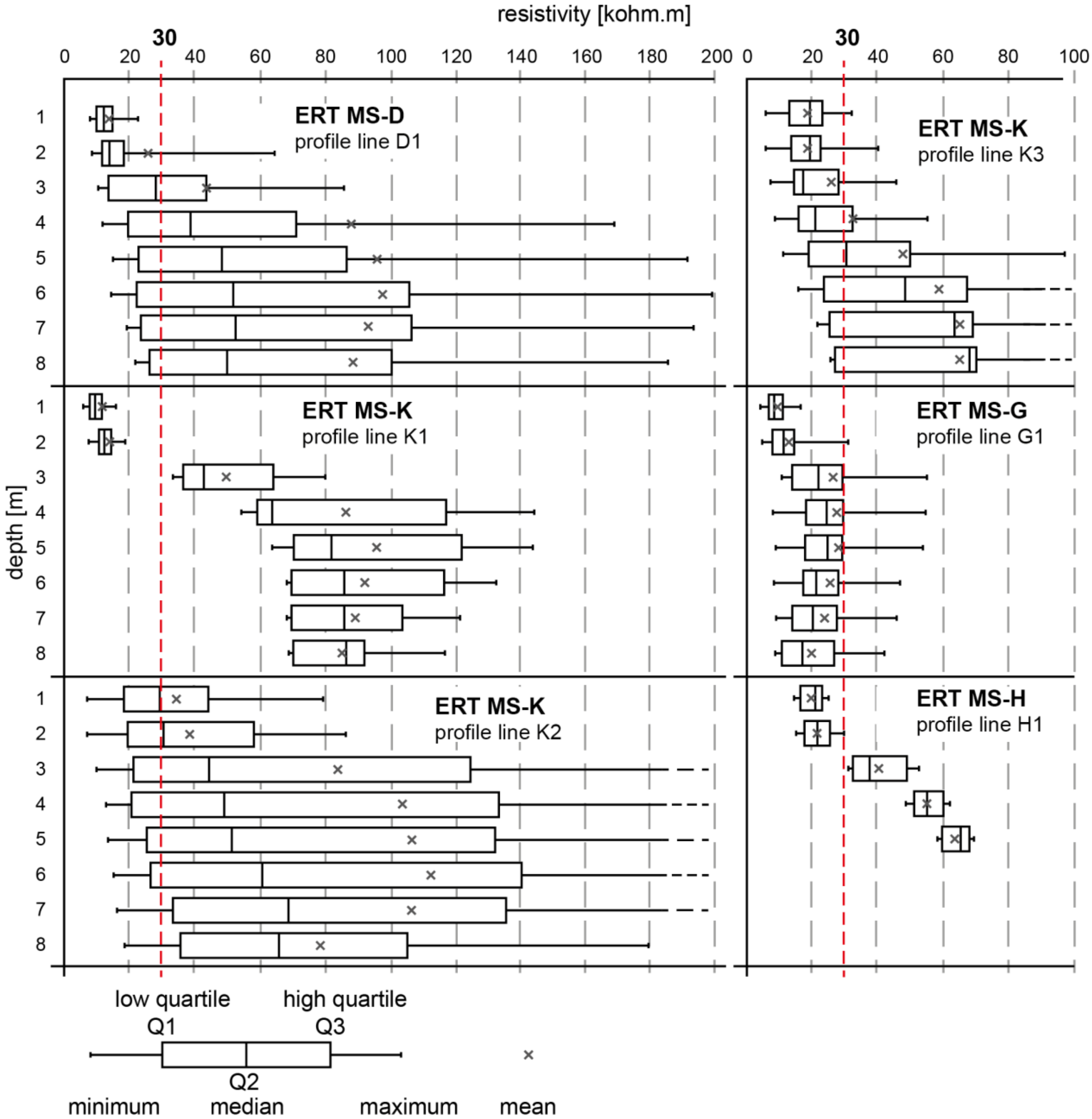

Figure 7: Boxplots of measured resistivity at depths from 0-8 m (distribution over the entire profile length). Value range for depth 1: 0< to ≤ 1m; 2: 1< to ≤ 2m and so on.

5 Discussion

5.1 General distribution of permafrost

Almost all of the measured BTS and GST temperatures point to the existence of permafrost in the zones along the upper glacier margins which have been subject to glacier retreat since the LIA maximum. This is confirmed by all 2D-geoelectic profiles (save MS-G) that indicate permafrost at some meters depth. At all four study sites permafrost layers with resistivities higher than 30 kohm.m occurred. Highest resistivities were found at the MS-K north face, followed by the MS-D site, while at the MS-G and MS-H the resistivities were lower and the border to the permafrost layers are not so pronounced (Fig. 6). The GST results support this resistivity order, with deeper WEqT temperatures beneath -5 °C at MS-K and WEqT between -5 and -3°C at the three other sites.

Long time (2004-2015) GST measurements in permafrost at a nearby mountain (Hochreichart 2416 m a.s.l.) show a general increase of the mean annual ground temperature (Kellerer-Pirklbauer, 2016). The mean annual temperature of 2013 at the Hochreichart site was an average value for the entire 2004-2015 period suggesting that our ground temperature data of 2013 for the Dachstein might be regarded as typical not only for a single year but at least for a decadal time-scale.

The permafrost model by Boeckli et al. (2012 a, b), which includes explanatory variables like annual air temperatures, potential incoming solar radiation and precipitation, fits quite well with our own field work results (Fig. 5-7). According to the GST/BTS classification defining temperatures < -3 °C as permafrost areas (Haeberli, 1973), all of our sites should be affected by permafrost in favorable conditions (Böckli et al., 2012a). The situation at MS-H is of particular local interest because of the touristic infrastructure with a cable car station on the top. Although the Boeckli et al. (2012a) model assumes permafrost only in very favorable conditions.for this site, the results at H1 clearly point to permafrost which is also underpinned by the temperature measurements.

At MS-K, the thinnest active layer and the highest resistivities of the deeper subsurface were found in the approximate middle of the vertical profiles, corresponding with the 1850 glacier surface. This is particularly well visible at the K1 profile. The flattening of the rockwall at K3 in the elevation of the 1850 surface probably enabled accumulation of infiltrated moisture and the development of massive ice below the surface (-2 to -10m). Generally higher resistivities (>50 kohm.m) were found in the part of the rockwall above the 1850 margin which has been ice-free for more than 150 years. At the ERT-sites near the present glacier surface (MS-K - K2, MS-D - D1, MS-G - G1 and MS-H - H1) which have been ice-free for a much shorter time, resistivities are lower and the active layer is thicker.

At D1 it is difficult to determine the historically highest surface of the glacier extent, because the glacier surface at the Dirndl mountain is influenced by the mentioned blowout depression at the footslope of this mountain. The investigated part of the rockwall at D1 was probably ice free even before 1850 (Simony, 1884) and thus exposed to atmospheric conditions for much longer than K2, G1 and H1. The absence of insulating glacier ice could be the reason for the well-established ice layers at the left and in the middle of the profile beneath the active layer. However, between those two frozen parts thawing processes occur with resistivities between 10 and 20 kohm.m, mirrored by a wet and fractured rock surface in the field.

5.2 Significance of ERT data for permafrost detection

ERT permafrost investigations in bedrock may be error-prone because the resistivity contrast is small between ice, air and certain rock types, as all three nearly behave as an electrical insulator with very high resistivities (Hauck and Kneisel, 2008). Furthermore, the resistivity values for subzero ground span a wide range from about 13 kohm.m to more than 30 kohm.m depending on the ice content (Hilbich et al., 2009). At all six ERT profile lines, areas with resistivities higher than 100 kohm.m up to 500 kohm.m (Table 1) were measured which, in all probability, represent frozen ground. These exceptionally high electrical resistivities could also be caused by air-filled cavities in the rock; due to karstification of the Dachstein limestone, the existence of caves can not be ruled out. However, the known caves usually occur in pronounced horizontal cave floors, and no cave mouths can be found at the elevation of the study sites. Furthermore, the geometrical distribution of high resistivities particularly at MS-K1 and the position of the resistivity anomalies beneath an active layer of +/- consistent depth make the interpretation as cavities extremely improbable. Furthermore, the interpretation is backed by GST and BTS temperatures.

The use of salt water and conductive grease at the drilled-in screws lowered contact resistances between electrodes and rock and provided satisfactory data quality in terms of RMS errors. The use of the DOI method showed, that mainly at high resistivity changes (between thawed and frozen layers) some areas with DOI > 0.2 occur and should be discussed with caution (Hilbich, 2009). However, these zones are in positions where they do not affect the general interpretation. On the whole, the DOI analyses showed that all ERT profiles are reliable. To exclude resistivity misinterpretations regarding frozen vs. unfrozen conditions, we performed resistivity measurements at a small scale geoelectric profile combined with temperature measurements at different depths. Krautblatter et al., (2010) performed systematic T/Res investigations in the laboratory and found a distinct resistivity increase with subzero temperatures. They determined 30 kohm.m as the threshold value from which on the rock (the very similar Wetterstein limestone) is very probably frozen. We were able to confirm these findings in a natural setting. The knowledge of the resistivity range of frozen and unfrozen rock *at our sites* puts the interpretation on a solid basis. The transition zone with a mixture of liquid water and ice with values between 13 and 30 kohm.m is characterized by the rapid increase of resistivity at the temperature change from positive to negative (starting around -0,5° C). During constant freezing and temperatures below -0.5 °C, values higher than 30 kohm.m. were measured.

5.3 Degradation or aggradation of permafrost?

Significant areas of the study region were affected by glacier recession and glacier surface lowering at the glacier forefield and the surrounding headwalls. The thermal regimes of surface ice and frozen ground can be interconnected and are influencing each other (Suter et al., 2001; Otto and Keuschnig, 2014). Our results prove the occurrence of permafrost in recently ice free rockwalls. An open question is if this permafrost has newly formed since glacier recession or if permafrost was already present under the ice?

At both vertical profiles MS-K1 and MS-K3 (Fig. 6) the largest area and highest resistivities of frozen rock is present near the 1850 glacier ice surface line. Frozen rock at some meters rock depth *below* the 1850 glacier surface level might (a) be due to permafrost aggradation due to the access of cold air since the beginning of glacier lowering. In this case, the glacier base should have been warm-based. (b) In case the glaciers in our study area are polythermal (i.e. of type d. on Fig. 2.6. in Benn & Evans, 2010), permafrost might exist under the cold-based areas of glacier ice. In this case, the active layer which developed since deglaciation would indicate current permafrost degradation. As the thermal conditions at the base of the Schladminger glacier are not yet known, this question cannot be definitively clarified and further research is needed. However, at profile MS-K1 the active layer thickness decreases from the lowest point of the profile upwards and reaches its minimum at the elevation of the 1850 line. This supports interpretation 'a' because the higher areas had more time for aggradation than the lower parts. If 'b' was right, we would expect the active layer to be thicker where the time span for permafrost meltdown was longer.

The higher parts of the vertical ERT profiles have been presumable ice free at least since the onset of the Postglacial as judged from general glacier evolution during the Holocene in the Eastern Alps (Wirsig et al., 2016). Thus, permafrost in these areas results from significantly different conditions than in the lower parts which have been ice free for a much shorter period of time; smaller, warmer permafrost layers with lower resistivities should be expected. This assumed pattern is realized at MS-K3 in an ideal way. However, the pattern is opposite at MS-K1 with much higher resistivity in the assumedly "younger" permafrost zone. The reason might be drier conditions above the 1850 line and the supply of meltwater below the line leading to more massive ice formations.

According to Magnin et al. (2017), statements regarding permafrost degradation (or aggradation) can only be made in combination with a time period. The authors simulated the long-term temperature evolution at three sites with different topographical settings between 3160 and 4300 m in the Mont Blanc massif, from the Little Ice Age (LIA) steady-state conditions to 2100. The simulation model was evaluated with borehole temperature and ERT measurements. Magnin et al. (2017) conclude that permafrost degradation has been progressing since the LIA.

As further changes in the shallow subsurface might become apparent after some years of observation, repeated measurements might clarify the question of degradation or aggradation of permafrost.

6 Conclusions and Outlook

The used methods have proven their applicability for permafrost mapping and have delivered information on permafrost distribution around the upper margins of retreating glaciers in the Dachstein area. Permafrost was found in all investigated north facing rockwalls between 2600 and 2800 m a.s.l. that were subject to glacier retreat since the LIA maximum. Permafrost preservation (or even aggradation, see below), is thus possible in favourable cold conditions in north faces with MAAT below -2.5 °C (2013). Slightly less shadowed sites oriented northwest and northeast show degradation effects with very heterogeneous subsurface ERT tomograms with frozen and unfrozen parts. At the only west-facing site no permafrost could be confirmed.

The ERT data are of good quality. The resistivity calibration by using data of a small scale ERT profile line proved to be a helpful method to delimit frozen from unfrozen rock which may aid the interpretation also in other study regions. The ERT interpretation is backed by GST and BTS data.

The existence of permafrost at the former ice-covered positions could be due to slow degradation of permafrost that already existed under polythermal glacier ice, or to aggradation of permafrost after glacier retreat. Some of the evidence points to aggradation which would be an important finding also for research in other study areas. However, without long-term observation this conclusion remains partly speculative.

To clarify the open questions of aggradation vs. degradation, repeated ERT and temperature measurements are necessary, together with temperature measurements at the glacier base to confirm warm-based or polythermal conditions.

7 Acknowledgements

This study was supported by the project ‘ROCKING ALPS – Rockfall and Weathering in the Eastern Alps’ financed by the Austrian Science Fund (FWF) through project no. FWF: P24244. Further thanks to the following organisations: Dachstein cable car company (E. Schnepfleitner and L. Traninger), Austrian Federal Forests, "snowreporter" for private climate and snow depth data, as well to G. K. Lieb for fruitfull discussions. Many thanks to Johannes Stangl, Eric Rascher, Reinhold Schöngrundner, Patrick Zinner and Eduard Rode for their help during fieldwork.

8 References

- Angelopoulos, M., Pollard, WH., Couture, N.: The application of CCR and GPR to characterize ground ice conditions at Parsons Lake, Northwest Territories. Cold Regions Science and Technology 85: 22-33, 2013.
- Benn, D.I., Evans, D.J.A.: Glaciers and Glaciation – Second Edition. Hodder Arnold Publication, 802 pp, 2010.

- Boeckli, L., Brenning, A., Gruber, S., Noetzli, J.: A statistical approach to modelling permafrost distribution in the European Alps or similar mountain ranges. – In: The Cryosphere 6 (1), S. 125–140, 2012a.
- Boeckli, L., Brenning, A., Gruber, S. and Noetzli, J.: Permafrost distribution in the European Alps: calculation and evaluation of an index map and summary statistics. – In: The Cryosphere 6, 807–820, 2012b.
- Brenning A., Gruber S. & Hoelzle M.: Sampling and statistical analyses of BTS measurements. Permafrost and Periglacial Processes 16: 383–393, 2005.
- Draebing, D., Haberkorn, A., Krautblatter, M., Kenner, R. and Phillips M.: Thermal and mechanical responses resulting from spatial and temporal snow cover variability in permafrost rock slopes. Permafrost and Periglacial Processes 28 (1):140-157, 2017a.
- Draebing, D., Krautblatter, M. and Hoffmann T.: Thermo-cryogenic controls of fracture kinematics in permafrost rockwalls. Geophysical Research Letters 44: 3535-3544, 2017b.
- Ebohon, B. and Schrott, L.: Modeling Mountain Permafrost Distribution. A New Permafrost Map of Austria. – In: Kane, D. und Hinkel, K. (ed.), Proceedings of the Ninth International Conference on Permafrost, Fairbanks, Alaska, 397–402, 2009.
- Fischer, A., Seiser, B., Stocker-Waldhuber, M., Mitterer, C., Abermann, J.: Tracing glacier changes in Austria from the Little Ice Age to the present using a lidar-based high-resolution glacier inventory in Austria. The Cryosphere, 9(2), 753-766, doi:10.5194/tc-9-753-2015, 2015.
- Frauenfelder, R.: Regional-scale modelling of the occurrence and dynamics of rockglaciers and the distribution of paleopermafrost, Schriftenreihe Physische Geographie, Glaziologie und Geomorphodynamik, University of Zurich, 2005.
- Gasser, D., Gusterhuber J., Krische, O., Puhr, B., Scheucher, L., Wagner T. and Stüwe K.: Geology of Styria: An Overview: Mitteilungen des Naturwissenschaftlichen Vereines für Steiermark, 139, 5–36, 2009.
- GBA - Geologische Bundesanstalt: Geologischen Karte der Republik Österreich, Bl. 96 Bad Ischl, Wien, 1982.
- Gobiet, A., Kotlarski, S., Beniston, M., Heinrich, G., Rajczak J. and Stoffel M.: 21st century climate change in the European Alps-A review. Sci. Total Environ., 493, 1138-1151, doi: 10.1016/j.scitotenv. 2013.07.050., 2014.
- Gruber, S., Peter, M. and Hoelzle, M.: Surface temperatures in steep Alpine rock faces—A strategy for regional-scale measurement and modelling, Proc. 8th Int. Conf. Permafrost, 1, 325– 330, 2003.
- Gubler, S., Fiddes J., Keller, M., and Gruber S.: Scale-dependent measurement and analysis of ground surface temperature variability in alpine terrain. The Cryosphere, 5, 431-443, 2011.
- Haeberli, W.: Die Basis-Temperatur der winterlichen Schneedecke als möglicher Indikator für die Verbreitung von Permafrost in den Alpen. – In: Zeitschrift für Gletscherkunde und Glazialgeologie 9 (1-2), 221–227, 1973.
- Haeberli, W.: Untersuchungen zur Verbreitung von Permafrost zwischen Flüelapass und Piz Grialetsch (Graubünden). Mitteilungen der Versuchsanstalt für Wasserbau, Hydrologie u. Glaziologie der ETH Zürich, 17, Zürich, 221, 1975.
- Haeberli, W., Hoelzle, M.: Application of inventory data for estimating characteristics of and regional climate-change effects on mountain glaciers: a pilot study with the European Alps. Annals of Glaciology, 21, 206-212, 1995.
- Haeberli, W., Wegmann, M. and Vonder Mühll D.: Slope stability problems related to glacier shrinkage and permafrost degradation in the Alps, Eclogae Geol. Helv., 90, 407– 414, 1997.
- Haeberli W., Hoelzle M., Paul F. and Zemp M.: Integrated monitoring of mountain glaciers as key indicators of global climate change: the European Alps. Annals of Glaciology 46, 150-160, 2007.
- Haeberli W., Huggel C., Paul F. & Zemp M.: Glacial responses to climate change. In: Treatise on Geomorphology, 13, Academic Press, San Diego: p. 152-175, 2013.

- Hartmeyer, I., Keuschnig, M., and Schrott, L.: Long-term monitoring of permafrost-affected rock faces – A scale-oriented approach for the investigation of ground thermal conditions in alpine terrain, Kitzsteinhorn, Austria. Austrian Journal of Earth Science, 105 (2): 128–139, 2012.
- Harris, C., Davies, M., and Etzelmüller, B.: The assessment of potential geotechnical hazards associated with mountain permafrost in a warming global climate, Permafrost and Periglacial Processes, 12, 145–156, 2001.
- Harris, C., Vonder Mühll, C., Isaksen, K., Haeberli, W., Sollid, J. L., King, L., Holmlund, P., Dramis, F., Gugliemin, M., and Palacios, D.: Warming permafrost in European mountains, Global and Planetary Change, 39, 215–225, 2003.
- Hauck, C.: Geophysical methods for detecting permafrost in high mountains, 171, ETH Zurich, Zurich, 1–204, 2001.
- Hauck, C., Vonder Mühll, D. and Maurer H.: Using DC resistivity tomography to detect and characterize mountain permafrost. Geophysical Prospecting 51:273–284, 2003.
- Hauck, C. and Kneisel, C.: Applied Geophysics in Periglacial Environments, University Press, Cambridge, 240 pp., 2008.
- Helfricht, K.: Veränderungen des Massenhaushaltes am Hallstätter Gletscher seit 1856. – Diplomarbeit, Institut für Meteorologie und Geophysik. Leopold-Franzens-Universität Innsbruck, 139, 2009.
- Hilbich, C., Marescot, L., Hauck, C., Loke, M.H. and Mäusbacher, R.: Applicability of Electrical Resistivity Tomography Monitoring to coarse blocky and ice-rich permafrost landforms. Permafrost and Periglacial Processes 20(3): 269–284. DOI: 10.1002/ppp.652, 2009.
- Humlum O.: The climatic significance of rock glaciers. Permafrost and Periglacial Processes 9: 375-395, 1998.
- Ishikawa, M.: Thermal regimes at the snow–ground interface and their implications for permafrost investigation. – In: Geomorphology 52 (1–2), S. 105–120, 2003.
- Kellerer-Pirklbauer, A.: A regional signal of significant recent ground surface temperature warming in the periglacial environment of Central Austria. In: Günther, F., Morgenstern, A. (Eds.), XI. International Conference On Permafrost – Book of Abstracts, 20–24 June 2016. Bibliothek Wissenschaftspark Albert Einstein, Potsdam, Germany, pp. 1025–1026, 2016.
- Kellerer-Pirklbauer A.: Potential weathering by freeze-thaw action in alpine rocks in the European Alps during a nine year monitoring period. Geomorphology 296 (2017) 113–131. http://dx.doi.org/10.1016/j.geomorph.2017.08.020, 2017.
- Kellerer-Pirklbauer A., Lieb G.K., Avian M. & Carrivick J.: Climate change and rock fall events in high mountain areas: Numerous and extensive rock falls in 2007 at Mittlerer Burgstall, Central Austria. Geografiska Annaler: Series A, Physical Geography, 94, 59-78, 2012.
- Kellerer-Pirklbauer, A., Lieb, G., Avian, M. and Gspurning J.: The Response of Partially Debris-Covered Valley Glaciers to Climate Change: The Example of the Pasterze Glacier (Austria) in the Period 1964 to 2006. Geografiska Annaler. Series A, Physical Geography, 90, 4, 269-285, 2008.
- Kern K., Lieb G.K., Seier G. & Kellerer-Pirklbauer A.: Modelling geomorphological hazards to assess the vulnerability of alpine infrastructure: The example of the Großglockner-Pasterze area, Austria. Austrian Journal of Earth Sciences, 105/2, 113-127, 2012.
- Kneisel, C., Hauck, C., Fortier, R., and Moorman, B.: Advances in geophysical methods for permafrost investigations, Permafrost Periglac., 19, 157–178, doi:10.1002/ppp.616, 2008.
- Knödel, K., Krummel H., and Lange, G. (ed.): Geophysik Handbuch zur Erkundung des Untergrundes von Deponien und Altlasten. Springer Verlag, Berlin, Band 3, 1102, 2005.
- Krautblatter, M. and Hauck, C.: Electrical resistivity tomography monitoring of permafrost in solid rockwalls, J. Geophys. Res.- Earth, 112, F02S20, doi:10.1029/2006jf000546, 2007.

- Krautblatter, M., Funk, D. and Günzel F.: Why permafrost rocks become unstable: a rock–ice-mechanical model in time and space. Earth Surface Processes and Landforms, 38, 8, 876–887, 2013.
- Krautblatter, M., Verleysdonk, S., Flores-Orozco, A., and Kemna, A.: Temperature-calibrated imaging of seasonal changes in permafrost rockwalls by quantitative electrical resistivity tomography (Zugspitze, German/Austrian Alps), J. Geophys. Res.-Earth, 115, F02003, doi:10.1029/2008JF001209, 2010.
- Krobath, M. and Lieb, G.: Die Dachsteingletscher im 20. Jahrhundert. – In: Brunner, K. (ed.), Das Karls-Eisfeld. Forschungsarbeiten am Hallstätter Gletscher. Wissenschaftliche Alpenvereinshefte, H. 38, Haus des Alpinismus, München, 75–101, 2004.
- Laxton, S. and Coates, J.: Geophysical and borehole investigations of permafrost conditions associated with compromised infrastructure in Dawson and Ross River, Yukon. *In*: Yukon Exploration and Geology 2010, K.E. MacFarlane, L.H. Weston and C. Relf (eds.), Yukon Geological Survey, 135-148, 2011.
- Lieb, G. and Schopper, A.: Zur Verbreitung von Permafrost am Dachstein (Nördliche Kalkalpen, Steiermark). – In: Mitt. naturwiss. Ver. Steiermark 121, 149–163, 1991.
- Lieb, G., Kellerer-Pirklbauer, A., Strasser U.: Effekte des Klimawandels im Naturraum des Hochgebirges. In: Fassmann H. and Glade T. (eds) (Hg.): Geographie für eine Welt im Wandel – 57. Deutscher Geographentag 2009 in Wien. 2012.
- Loke, M.H.: Electrical imaging surveys for environmental and engineering studies, a practical guide to 2-D and 3-D surveys. Copyright by M.H. Loke, Penang (Malaysia), 1999.
- Magnin, F., Josnin J., Ravanel L., Pergaud J., Pohl B., and Deline P.: Modelling rock wall permafrost degradation in the Mont Blanc massif from the LIA to the end of the 21st century. The Cryosphere 11, 1813–1834, 2017.
- Magnin, F., Krautblatter, M., Deline, P., Ravanel, L., Malet E. and Bevington, A.: Determination of warm, sensitive permafrost areas in near-vertical rockwalls and evaluation of distributed models by electrical resistivity tomography. Journal of Geophysical Research 120, 5, 745–762, 2015. 10.1002/2014JF003351, 2015.
- Marescot, L., Loke, M.H., Chapellier, D., Delaloye, R., Lambiel, C. and Reynard, E.: Assessing reliability of 2D resistivity imaging in permafrost and rock glacier studies using the depth of investigation index method. Near Surface Geophysics 1(2): 57–67, 2003.
- Matsuoka, N. and Sakai H.: Rockfall activity from an alpine cliff during thawing periods. Geomorphology, 28, 3-4, 309-328, 1999. doi:10.1016/S0169-555X(98)00116-0, 1999.
- Moser, R.: Dachsteingletscher und deren Spuren im Vorfeld, Musealverein Hallstatt, Hallstatt, 143, 1997.
- Österreichischer Alpenverein: Jahrbuch des Österreichischen Alpenvereins (Alpenvereinszeitschrift). Bd. 83, Universitätsverlag Wagner, Innsbruck, 158 S., 1958.
- Oldenburg, D.W. and Li, Y.G.: Estimating depth of investigation in dc resistivity and IP surveys. Geophysics 64(2): 403–416. DOI: 10.1190/1.1444545, 1999.
- Otto, J and Keuschnig, M.: Permafrost-Glacier Interaction – Process Understanding of Permafrost Reformation and Degradation. Austrian Permafrost Research Initiative. Final Report, Chapter: 1, Publisher: ÖAW - Austrian Academy of Sciences, Editors: Martin Rutzinger, Kati Heinrich, Axel Borsdorf, Johann Stötter, 3-16, 2014.
- Paul, F., Kääb, A., Maisch, M., Kellenberger, T. W., and Haeberli, W.: Rapid disintegration of Alpine glaciers observed with satellite data, Geophys. Res. Lett., 31, L21402, doi:10.1029/2004GL020816, 2004.
- Ravanel, L. And Deline P.: Climate influence on rockfalls in high-Alpine steep rockwalls: The north side of the Aiguilles de Chamonix (Mont Blanc massif) since the end of the 'Little Ice Age'. *The Holocene* 21, 2, 357-365. doi: 10.1177/0959683610374887, 2011.

- Rödder, T. and Kneissel, C.: Permafrost mapping using quasi-3D resistivity imaging, Murtèl, Swiss Alps. Near Surface Geophysics, 10, 2, 117 – 127, 2012.
- Sattler, K., Keiler, M., Zischg, A., and Schrott, L.: On the Connection between Debris Flow Activity and Permafrost Degradation: A Case Study from the Schnalstal, South Tyrolean Alps, Italy. Permafrost and Periglacial Processes, 22 (3): 254-265, 2011.
- Schmid, M., Gubler, S., Fiddes, J. and Gruber, S.: Inferring snowpack ripening and melt-out from distributed measurements of near-surface ground temperatures. – In: The Cryosphere 6 (5), S. 1127-1139, 2012.
- Schopper, A.: Die glaziale und spätglaziale Landschaftsgenese im südlichen Dachstein und ihre Beziehung zum Kulturlandausbau. – Diplomarbeit. Karl-Franzens- Universität Graz, 161, 1989.
- Schrott, L. and Sass, O.: Application of field geophysics in geomorphology: Advances and limitations exemplified by case studies. – In: Geomorphology 93: 55-73, 2008.
- Simony, F.: Photographische Aufnahmen und Gletscheruntersuchungen im Dachsteingebirge. – In: Mitteilungen des Deutschen und Österreischischen Alpenvereins, 10, S. 314-317, 1884.
- Simony, F.: Das Dachsteingebiet. Ein geographisches Charakterbild aus den Österreichischen Nordalpen, Hölzel, Wien, 152, 1895.
- snowreporter (2013): snowreporter Telekommunikationssysteme GmbH, Klimadatensatz Dachstein, Graz. – E-Mail, 10/2013.
- Stiegler, C., Rode, M., Sass, O. and Otto, J.: An Undercooled Scree Slope Detected by Geophysical Investigations in Sporadic Permafrost below 1000 M ASL, Central Austria. Earth Surface Processes, 25, 3, 194–207, 2014.
- Supper, R., Ottowitz, D., Jochum, B., Römer, A, Pfeiler, S., Kauer, S., Keuschnig, M. and Ita, A.: Geoelectrical monitoring of frozen ground and permafrost in alpine areas: field studies and considerations towards an improved measuring technology, Near Surface Geophysics, 2014, 12, 93-115, 2014.
- Suter, S., Laternser, M., Haeberli, W., Frauenfelder R. and Hoelzle, M.: Cold firn and ice of high altitude glaciers in the Alps: measurements and distribution modelling Journal of Glaciology, 47 (156): 85–96, 2001.
- Wegmann, M., Gudmundsson G. and Haeberli, W.: Permafrost changes and the retreat of Alpine glaciers: A thermal modelling approach, Permafrost Periglacial Processes, 9, 23–33, 1998.
- Wirsig C., Zasadni J., Christl M., Akçar N., Ivy-Ochs S.: Dating the onset of LGM ice surface lowering in the High Alps, Quaternary Science Reviews, 143 (2016) 37-50, 2016.
- Zemp, M., Paul, F., Hoelzle, M., and Haeberli, W.: Glacier fluctuations in the European Alps 1850–2000: an overview and spatiotemporal analysis of available data, in: The darkening peaks: Glacial retreat in scientific and social context, edited by: Orlove, B., Wiegandt, E., and Luckman, B., University of California Press, in press, 2006.